INTERNATIONAL JOURNAL OF ENERGY RESEARCH
Int. J. Energy Res. (2009)
Published online in Wiley InterScience
(www.interscience.wiley.com). DOI: 10.1002/er.1595

SHORT COMMUNICATION

A small, high-efficiency diesel generator for high-altitude use in Antarctica

Shane Hengst[1,*,†], D. M. Luong-Van[1], J. R. Everett[1], J. S. Lawrence[1,‡], M. C. B. Ashley[1], D. Castel[1,2] and J. W. V. Storey[1]

[1]*School of Physics, University of New South Wales, Sydney, NSW 2052, Australia*
[2]*Institut Supérieur de l'Électronique et du Numérique, 20 rue Cuirassé Bretagne, CS 42807-29228 Brest Cedex 2, France*

SUMMARY

We have characterised a small, high-efficiency diesel generator selected to power remote experiments on the Antarctic plateau at altitudes of up to 5000 m. We describe the design of an environmental chamber to simulate these high altitudes and present an experimental investigation of the engine operation at high altitude on Jet A-1, comparing this to the engine's performance at sea level. Although attention must be paid to the provision of adequate cooling, no modification to the engine itself is required. Our final system provides very high reliability and produces 1500 W of electrical power with a fuel consumption of 280 g kWh^{-1}. A bank of ultracapacitors is used to start the engine in the cold environment of Antarctica. We describe the low-temperature operation and survival tests that we performed on the ultracapacitors and the engine. Copyright © 2009 John Wiley & Sons, Ltd.

KEY WORDS: diesel engine; high altitude; antarctica; remote generation

1. INTRODUCTION

The Antarctic plateau is a vast, largely unexplored region in East Antarctica. Most of it is at an elevation of over 3000 m, with Dome A being the highest point at 4093 m. Scientific interest in the Antarctic plateau is growing, both for the historical climate information that can be gained from deep ice cores [[1], references therein], and the potential it offers for new astronomical observatories with 'space-like' observing conditions [[2], references therein]. Permanent stations now exist at the South Pole (on the edge of the plateau), Vostok and Dome C, with new stations under construction at Dome A and Dome F.

*Correspondence to: Shane Hengst, School of Physics, University of New South Wales, Sydney, NSW 2052, Australia.
†E-mail: shane@phys.unsw.edu.au
‡Present address: Macquarie University/Anglo-Australian Observatory, Sydney, NSW, Australia.

Contract/grant sponsor: Australian Research Council

Received 12 February 2009
Accepted 13 June 2009

To facilitate the exploration of these, and other high Antarctic sites, we have developed a system of small, high-efficiency diesel generators. Six of these generators are installed in PLATO, the PLATeau Observatory [3–5], a robotic observatory that was deployed to Dome A, in January 2008 by the Polar Research Institute of China. PLATO is measuring the atmospheric conditions at Dome A in order to gather information for future large astronomical telescopes. PLATO also provides a scientific platform for small telescopes and other experiments [6,7]. The PLATO facility itself is composed of two modules, each built into a 10-foot shipping container: an instrument module with a flexible computer-controlled system for the instrument suite [8]; and an engine module that provides the primary power during the winter months [9].

There are five astronomical instruments on PLATO, each of which is designed to run on less than 100 W (average) power. Electrical power is also required for heaters to keep the instruments warm and to provide additional heat to the instrument module itself. Yang *et al.* [3] present a detailed description of PLATO and first season (2008) results for the above-mentioned instruments. Lawrence *et al.* [5] present a detailed description of PLATO's power generation and control systems, together with an overview of the system performance for 2008.

PLATO must operate unmanned throughout the year because of the remoteness of Dome A. Except for a period of a few weeks in January each year when the annual servicing missions take place, communications with the observatory are only possible via the Iridium satellite network. Thus, the power generation system needs to be maintenance-free for a period of 11 months.

During the summer months, when the sun is above the horizon, PLATO can be powered largely by an array of solar panels. However, moving into winter there is progressively less sun available and for approximately 3.5 months of the year the sun is continuously below the horizon. Unlike the Antarctic coast, where wind turbines can provide large amounts of power, the plateau is remarkably free of wind. Dome A has possibly the lowest average wind speed of any place on earth [10], making wind power impractical.

Several other possible power sources are discussed in Lawrence *et al.* [11]. Perhaps the most promising in the longer term are fuel cells. These have been tested in an Antarctic environment [12] but the technology is still relatively immature. In addition, the energy density of the most suitable fuel, methanol, is less than half that of jet fuel.

These arguments lead to the selection of diesel engines to augment the solar power. Six 4-volt 320 AHr lead-acid batteries are used to provide temporary energy storage. To provide redundancy and increase the flexibility of PLATO's power system, six independent engines are used in PLATO [5]. The factors leading to the choice of Jet A-1 fuel are described in Section 2.3. However, in principle almost any hydrocarbon fuel could be used, including bio-diesel or other renewable fuel.

Dome A, the highest point on the Antarctic plateau has a physical elevation of 4093 m above sea level. However, the low temperatures in Antarctica lead to a reduced atmospheric scale height; i.e. the atmospheric pressure falls off more rapidly with altitude than at a temperate site. Thus, the average pressure at Dome A is about 575 hPa [10] (roughly half that at sea level), corresponding to a pressure altitude of 4530 m. The average summertime temperature at Dome A is about -35°C, dropping to as low as -90°C in winter. This is well below the freezing point of any commonly available fuel. The design philosophy of PLATO is therefore for the engines to keep themselves and their fuel warm throughout the year using waste engine heat. The engine must be able to start reliably from cold in the summer time, but thereafter the engines are in a warm, highly insulated, temperature-regulated environment. However, should all the engines fail during the winter, they may need to survive temperatures as low as -90°C before the service crew arrives the following January.

The development of the PLATO engine system therefore consisted of the following steps:

- Selection of an appropriate engine and alternator.
- Selection of an appropriate fuel.
- Measurement of the engine performance at high (simulated) altitude.

DOI: 10.1002/er

- Design and testing of a low-temperature starting system.
- Verification of the survival of the engine system at extreme low temperatures.

These steps are detailed in the following sections.

2. DESIGN OF THE GENERATOR SYSTEM

2.1. Design criteria

2.1.2. Engine selection. For our purposes, only a small amount of power is needed ($\sim$1.5 kW) making turbocharging unnecessary. The simplest and lowest cost choice is thus that of naturally aspirated single-cylinder diesel engine.

The engine we selected is a commercially available Hatz 1B30 single-cylinder, naturally aspirated diesel four-stroke with a displacement of 347 ml. It is a direct-injection, air-cooled engine with a bore of 80 mm and stroke of 69 mm, and a compression ratio of 21.5. The design speed of operation is 1500–3600 rpm. At 3600 rpm the engine can produce 5000 W at sea level. However, the minimum brake specific fuel consumption (BSFC) is at 2200 rpm, and the engine wear rate is much reduced at this lower speed. Allowing for the lower atmospheric pressure at Dome A, we expect a maximum power output of $\sim$2 kW at 2200 rpm. In practice, we would plan to run the engine at still lower power levels, partly to ensure complete combustion and reduce pollution to an absolute minimum.

The choice of an air-cooled engine was also motivated by the desire to keep everything as simple as possible. The standard engine-cooling fan was retained, and the warm air passing over the cylinder head allowed to circulate within the engine module. The overall internal temperature of the engine module is regulated by a separate thermal management system [8].

2.1.2. Engine lubrication. The crankcase oil selected was Mobil 1 Delvac 5w-40, chosen for its low pour point of -45°C and for its recommended use in high performance applications of heavy-duty diesel engines [13].

For operation in PLATO, each engine's running time is much longer than the manufacturer's recommended service interval of 200 h. In order to achieve this, the engine lubrication system has been extensively modified. Each of the two banks of three engines has a 60 l external oil tank. Oil from the tank is continuously pumped into each engine with a Thomas Magnete LHP27 metering pump at a rate of approximately 11 cc min^{-1} at 3 Hz. At each crankcase, a simple overflow pipe is used to return the excess oil to the storage tank. Large-area filters are used to clean the oil.

2.2. Electrical output

Although small generator sets are already commercially available, including some with diesel engines, they are normally directly coupled to 50/60 Hz alternators producing a nominal 220/110 V AC. There are two main reasons why we chose not to take this path.

1. Such engines must run at 3000 or 3600 rpm, at which speed BSFC is considerably higher and the life of the engine is greatly reduced.
2. The alternators used are normally relatively inefficient, especially where voltage regulation via a slip-ring field excitation is used.

Given that PLATO would be operating alone for 11 months, we decided to deploy two different types of generator in order to maximise the chance of success. The generators chosen were

- A three-phase brushless bearing-less alternator made by eCycle. These units are lightweight and compact, with the NdFeB permanent magnet rotor mounted directly onto the crankshaft. The output of the alternator is rectified with an IR 70MTKB diode bridge. The manufacturer quotes an efficiency of about 90% under our operating conditions, not including the losses in the diode bridge.
- A DC servo motor MSS-22 made by Mavilor. This disc motor has very high efficiency (both as a motor and as a generator) as it does not suffer from iron loss.

DOI: 10.1002/er

During engine testing, only an eCycle alternator was used, as its compact design made it easier to install in the test chamber. For these tests we used a unit with a voltage constant of $40\,\mathrm{V\,krpm^{-1}}$.

2.3. Fuel selection

The high cost (typically \$4–\$10 $\mathrm{kg^{-1}}$) of transporting fuel to and across Antarctica implies that the optimum strategy is to use a fuel of the highest possible energy density. Similarly, the environmental issues associated with transport logistics tend to outweigh the environmental effects of burning the fuel itself, leading to the selection of diesel or jet fuel—the highest energy-density fuels that are readily available. Jet fuel is cleaner burning and has a significantly lower freezing point (or, more accurately, pour point) than even SAB (Special Antarctic Blend) diesel, and was therefore chosen for our application.

There are many types of jet fuels available [14]. The most common is Jet A-1, a kerosene grade that contains a complex mixture of higher-order hydrocarbons. Jet A-1 (and its US counterpart Jet A) is widely used for commercial aircraft with turbine engines, while JP-8 is used for military aircraft. JP-8 is essentially Jet A-1 but with three additives to reduce ice build-up, corrosion and electric charge [15]. We chose Jet A-1 because of its ready availability in Antarctica.

The use of jet fuel in diesel engines is not unusual. NATO's Single Fuel Concept (SFC), for example, specifies JP-8 (or NATO code: F-34) as the single fuel to be used for all of their land and air military transports. Also, Jet A-1 has previously been used for a bank of six diesel engines for the winter operation of the Italian Antarctic coastal station at Terra Nova Bay [16].

As Jet A-1 is primarily used for turbine engines, it is usually combined with additives before use in compression-ignition engines. Diesel oil has a typical cetane index of about 55, corresponding to a shorter ignition delay than Jet A-1 (or JP-8, which has a cetane index closer to 47). Jet A-1 will thus perform better as a diesel fuel if it is mixed with a cetane enhancer and an oil to improve its lubrication properties. However, as the Hatz 1B30 is already specified for use with Jet A-1, we elected not to add a cetane enhancer. We mixed the fuel with $\sim$2% fully synthetic 'Racing 2T' two-stroke oil to provide lubrication for the fuel pump and the injection system [17]. In order to keep the fuel warm during the winter months, the fuel in PLATO is kept inside the well-insulated engine module in a 40001 aluminium tank. The tank is reinforced by aluminium webs that also act to conduct heat to the fuel at the bottom of the tank. Fuel is pumped from the bottom of the tank with a Thomas Magnete LHP27 metering pump and passes through a large-area filter on its way to the engine.

In Table I we present typical values of the basic properties of Jet A-1, automotive diesel and SAB. There is no specified value for the cetane index of Jet A-1, but it is assumed to be similar to that of JP-8. Jet fuel properties also vary from source to source [26].

2.4. Engine starting

The Hatz engine is electromechanically started in the usual way, with a solenoid engaging the starter

Table I. Fuel properties of Jet A-1, Automotive Diesel and Special Antarctic Blend (SAB) [18–24].

Fuel	Density at 15°C ($\mathrm{kg\,l^{-1}}$)	Energy density ($\mathrm{MJ\,kg^{-1}}$)	Cetane index (–)	Max. viscosity ($\mathrm{mm^2\,s}$)@40°C	Freezing point (°C)	Flash point (°C)	Auto-ignition point (°C)
Jet A-1	$\sim$0.81	42.8 (min)	$\sim$47*	$\sim$2	<-47	$>$38.0	$\sim$240
Diesel	0.85 (max)	45.6	$\sim$55	$\sim$6	<-35	$>$60.0	$\sim$240
SAB Diesel	$\sim$0.82	46.4	$\sim$51	$\sim$7	<-35	$>$61.5	$\sim$240†

*Cetane Index (CI) quoted for Jet A-1 is actually the CI for JP-8 [25].
†Since Diesel and SAB Diesel are chemically similar then the auto-ignition temperatures are also similar.

DOI: 10.1002/er

motor pinion with the ring gear on the crankshaft. The peak current required is 300 A at 12 V, and the motor will normally start within 1–2 s.

In order to improve the reliability of starting at low temperatures, we use ultracapacitors in place of the usual lead-acid battery. This is because the internal resistance of lead-acid batteries rises rapidly with decreasing temperature, whereas ultracapacitors can deliver thousands of amperes even at -40°C. The ultracapacitors are type BCAP3000 manufactured by Maxwell under the trade name Boostcap; each capacitor is about the size of a soft-drink can and is rated at 3000 F, 2.7 V.

For PLATO, two banks of ultracapacitor are used: one of 500 F (6×3000 F capacitors in series) and the other of 1000 F (12×3000 F capacitors in series-parallel). The capacitor banks are charged with a 12 V DC/DC converter that is current-limited to 9 A. Each of the capacitors is shunted with a simple clamp circuit that limits the voltage across it to a conservative value of 2 V. The clamp circuit must be able to pass the full charging current (9 A) from the time it turns on for as long as it takes for the sum of the voltages across the capacitors to rise to the value set by the DC/DC converter—in this case 12.0 V. In addition, the circuit creates a shunt current path of 45 mA. This is ten times the leakage current of the capacitors, and thus helps to equalise the voltage across each one. This shunt current will also discharge the capacitors with a time constant of 19 h after the system has been powered down.

3. COLD TEMPERATURE TESTS

Several important cold-temperature tests were carried out to ensure that the system would operate satisfactorily in Antarctica and would survive both the low temperatures that would be experienced during transport and the even lower temperatures that would occur during winter in the event of a power failure. The tests were carried out in a Forma Scientific Model 8558 laboratory freezer.

3.1. Fuel separation

Because of the possibility that the fuel for PLATO will freeze at least once before being used by the engines, it was important to determine if this would cause any separation of the Jet A-1 and oil. A sample of the fuel mix was placed in the laboratory freezer and cooled to -90°C. The freezing point of the fuel mix was determined to be about -57°C, somewhat lower than the nominal Jet A-1 freezing point. Upon thawing, the fuel mix showed no visible stratification between the jet fuel and the two-stroke oil.

3.2. Engine survival

The engine manufacturer, Hatz, Germany, specifies that the Hatz 1B30 engine has a minimum storage temperature of -46°C. However, with the possibility of the engine experiencing much lower temperatures than this in Antarctica, it was important to determine what, if anything, would happen if it were exposed to extreme cold. Problems that might be anticipated include permanent distortion of metal components and cracking of elastomeric seals. A 1B30 engine was frozen to -90°C overnight in the laboratory freezer and then allowed to stand at room temperature to thaw. Once thawed, the engine was found to restart successfully and to perform well. No oil leaks or other issues were discovered.

3.3. Ultracapacitor current delivery

A BCAP3000 ultracapacitor was charged to 2.0 V and discharged at various currents (5, 62.5 and 121A) while monitoring the charge and discharge time. This test was carried out as a function of temperature, with little change in behaviour being evident between room temperature and -40°C. At -46°C the ultracapacitor made an abrupt transition from capacitor to insulator, presumably because the electrolyte froze.

The internal resistance of the ultracapacitor was measured at -40°C by measuring the change in voltage across its terminals when the current drawn from it was switched from 0 to 107 A. The resulting value of 0.19 milliohm is consistent with the data sheet value of 0.29 milliohm $\pm 35\%$.

3.4. Ultracapacitor and clamp circuit survival

A BCAP3000 ultracapacitor was tested at room temperature then frozen to -90°C. Upon thawing

DOI: 10.1002/er

the capacitor was found to have the same capacitance and discharge current capability as before. The clamp circuit was similarly (mis) treated, and was also found to perform flawlessly on thawing to −40°C. This gave us confidence that the ultracapacitor bank would survive a winter without heat, and be capable of starting the engines the following spring.

4. ENGINE TEST RIG

4.1. Mechanical

In order to simulate the low atmospheric pressure of Dome A in the laboratory, an environmental chamber was designed and built with the capability of maintaining a constant pressure down to half an atmosphere with the engine running at full power. The chamber consists of a base plate and a bell-jar made from mild steel. The base plate is a circular disk, 30 mm thick, with an outer diameter of 1100 mm. The bell-jar has a wall thickness of 5 mm, with a welded dome-shaped top and a welded bottom flange. Two lifting hooks were welded on either side of the bell-jar to accommodate a crane. The bell-jar is sealed over the base plate via an O-ring. See Figure 1.

An 8 $m^3 min^{-1}$ Longtech LTV-100 Roots blower, driven by a Teco CNS-C4088 15 kW three-phase electric motor, extracts air from the chamber and vents it outside the building. The flow rate was chosen to be an order of magnitude greater than the rate at which the engine consumed air, so that the engine exhaust was well diluted before reaching the Roots blower. Air was continuously introduced into the chamber via an air-filter box and butterfly valve. The butterfly valve was manually adjusted to set the desired pressure within the chamber.

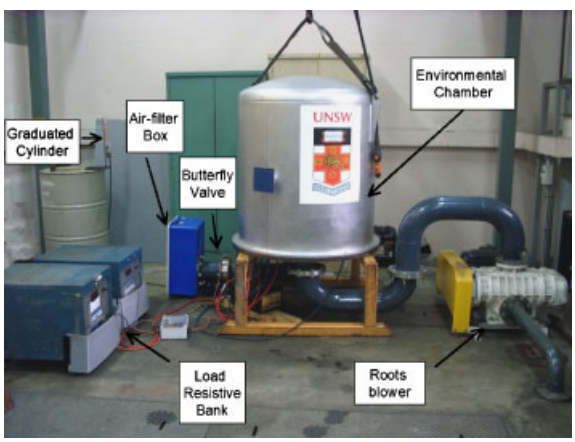

Figure 1. Engine test rig. The air flows through the air-filter box to the environmental chamber. The rate of airflow is controlled by the butterfly valve. The Roots blower runs at constant speed, pumping air from the environmental chamber.

The engine was attached via rubber isolation dampeners to the base plate of the chamber. See Figure 2. The eCycle alternator was directly attached to the engine crankshaft, and the three-phase electrical output coupled via a diode bridge to a pair of resistor load banks. The engine breathed the reduced pressure air from inside the chamber, while the exhaust exited via a diffuser that allowed the exhaust gases to be well mixed with the main airflow before reaching the Roots blower.

A motor-driven lead screw was attached to the engine governor lever in order to control the speed of the engine. The actuator was mounted on the engine plate and was electrically controlled via a switch that was external to the chamber.

Fuel consumption was measured using an externally mounted graduated cylinder, which delivers fuel via a fuel line that passes through a seal in the base plate to the engine. By having the fuel-feed system mounted externally to the pressure chamber,

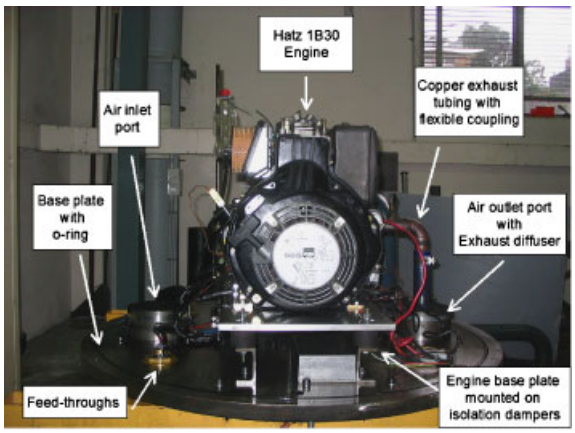

Figure 2. Engine mounted on base-plate of the environmental chamber with peripherals.

DOI: 10.1002/er

less vibration was coupled to the graduated cylinder, thus allowing a more accurate reading of the fuel level. The graduated cylinder could be read by eye to ± 0.5 ml. Typical consumption during a run was 60 ml, leading to a formal error in the amount of fuel consumed of $\pm 2\%$.

4.2. Data acquisition

Several sensors were placed on and around the engine to monitor various engine parameters. The processed signals from the sensors were fed into a desktop PC running Windows XP.

K-type thermocouples were used to measure the temperatures of the ambient air, oil sump, cylinder head, exhaust gas, alternator and the intake air. Two Motorola MPX4115AP pressure sensors with a specified accuracy of $\pm 1.5\%$ were placed inside the chamber. Output from the thermocouples, pressure sensors, and the resistor load bank sensors were all processed by ADAM modules connected via a serial device server (Moxa NPort 5410) to the Desktop PC. The formal accuracy of the temperature measurement is about 0.1°C and that of the voltage and current 0.1%. The engine speed was also monitored by a tachometer directly connected to the serial device server. All information received from sensors was then processed and logged in real time by the National Instrument's software package, LabVIEW. Virtual Instrument (VI) software created in LabVIEW allowed all parameters and data to be displayed on the computer monitor in real time and also stored to an output file. The output '*.csv' file was packed by the VI with the first column being allocated to time and subsequent columns being the calibrated sensor values.

The file was loaded into Matlab to produce plots of the engine sensor values as a function of time (see Section 4.3). Matlab was used to calculate the means of the pressure, voltage, current and engine speed over the duration of the run. These average values were imported into Microsoft Excel to calculate the overall BSFC.

4.3. Test procedure

The engine was started and stopped at a variety of simulated altitudes. It was found to start reliably, from ambient (typically ~ 25°C), at altitudes of more than 5000 m. Tests of starting at low temperatures were not performed, as the concept of PLATO is that one engine is always running, and thus keeps the other engines warm.

The majority of tests were conducted at a fuel injection timing of 18° crank angle before top dead centre (CA BTDC). Tests were made under otherwise identical conditions at both sea-level atmospheric pressure (1000 hPa) and at a pressure of about 540 hPa (hereinafter described as 'at altitude'). The corresponding pressure altitude is 5000 m, which is well above that of Dome A. Each test was allowed to go for no more than 10 min in order to avoid possible overheating of the engine within the chamber.

The engine speed was set at discrete intervals from 1600 to 3200 rpm and the load varied from 50 W up to 3 kW. At each setting, the following parameters were recorded:

- Fuel consumed
- Load-bank voltage and current
- Exhaust gas temperature

A typical data set for an engine test is presented in Figures 3–5. This particular engine test was conducted at a simulated altitude of 4500 m and at a crankshaft speed of 2200 rpm. The engine runtime was 390 s (5.5 min).

The ambient temperature inside the chamber was observed to increase by about 10°C during the

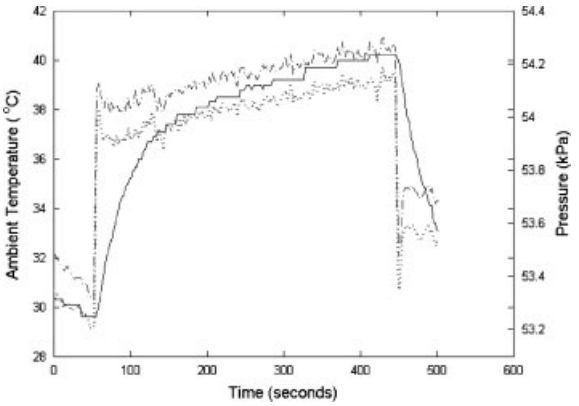

Figure 3. Ambient temperature (solid line) and air pressure (dotted and dot-dashed lines) inside the chamber during a typical test run.

DOI: 10.1002/er

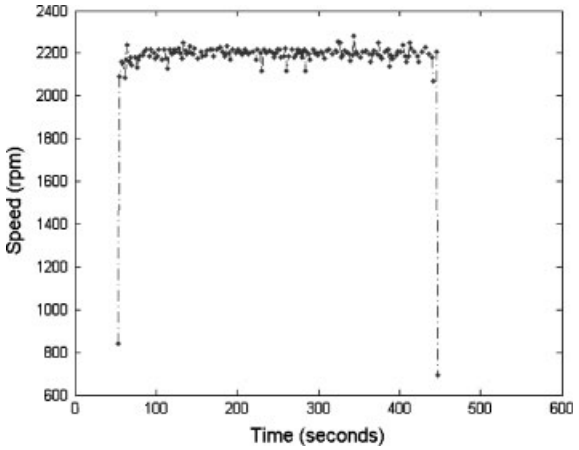

Figure 4. Engine speed during a typical test run showing the stability of the engine governor.

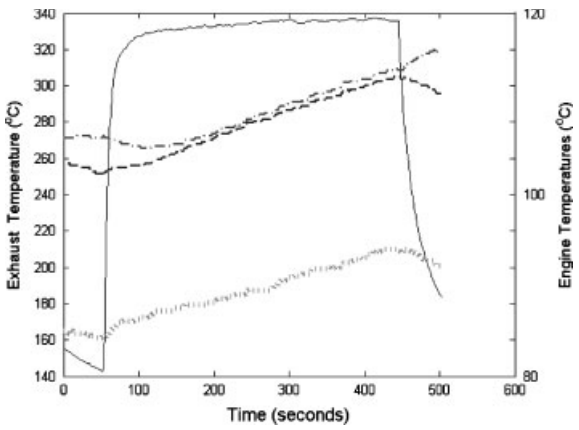

Figure 5. The exhaust gas temperature (left scale, solid line), and other engine temperatures (right scale) during a typical test run. The engine temperatures are: the cylinder head (dot-dashed line); the generator (dashed line) and the oil sump (dotted line).

operation of the engine. This increase in intake air temperature resulted in a small decrease in power output from the engine as the run progressed and a slight increase in the chamber air pressure (see Figure 3). However, the engine governor was able to keep the engine speed very constant, as shown in Figure 4.

The cylinder head, generator, oil sump and exhaust gas temperatures (Figure 5) were also monitored so that the observer could initiate an immediate shutdown of the engine and the Roots blower in the event of a serious system failure.

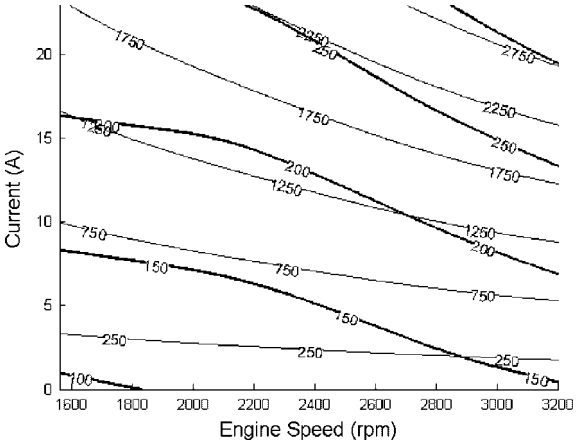

Figure 6. Sea level engine map, showing the exhaust gas temperature (°C, thick line) and power output (W, thin line) as a function of current (*y*-axis) and engine speed (*x*-axis).

The Hatz engine is supplied for the EPA market with an injection timing of 18° CA BTDC, and for the non-EPA market with 13° CA BTDC. Although we expected the advanced injection timing would give better performance at altitude, we nevertheless conducted a further set of tests at an injection timing of 13° CA BTDC. These tests were conducted at a fixed engine speed of 2200 rpm.

5. RESULTS AND DISCUSSION

5.1. Engine map data and engine efficiency

Figures 6 and 7 are smoothed engine contour maps at sea level and at altitude, respectively. Each contour map shows exhaust gas temperature and the total power as a function of current (*y*-axis) and engine speed (*x*-axis). The current is directly proportional to the torque developed by the engine.

The engine maps of Figure 6 and 7 show a greatly increased exhaust temperature at altitude. This is to be expected: for a given power output and rpm, a specific amount of thermodynamic work has to be performed each cycle. At altitude, only 54% of the mass of air is present in the

DOI: 10.1002/er

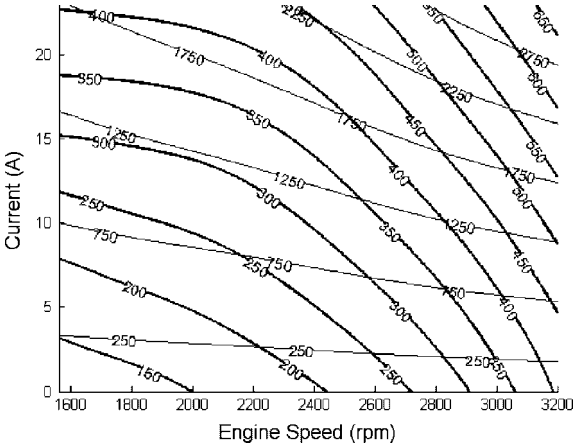

Figure 7. At altitude engine map, showing the exhaust gas temperature (°C, thick line) and power output (W, thin line) as a function of current (*y*-axis) and engine speed (*x*-axis).

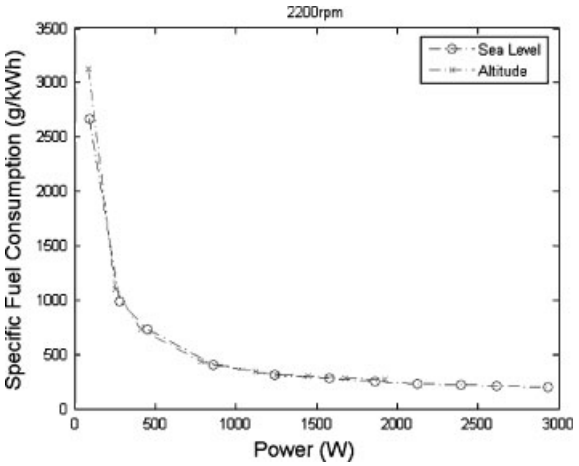

Figure 8. Brake specific fuel consumption ($g\,kWh^{-1}$) as a function of power at a fixed engine speed of 2200 rpm.

cylinder compared to sea level, and so this air must undergo a greater temperature excursion to perform the same work. In addition, the amount of air available for cooling is also reduced by nearly 50%.

In Figure 8, the power that was recorded was the electrical output power from the alternator, and thus included the alternator and rectifier losses. BSFC figures (in $g\,kWh^{-1}$) are therefore an overall fuel-to-electricity efficiency. At an

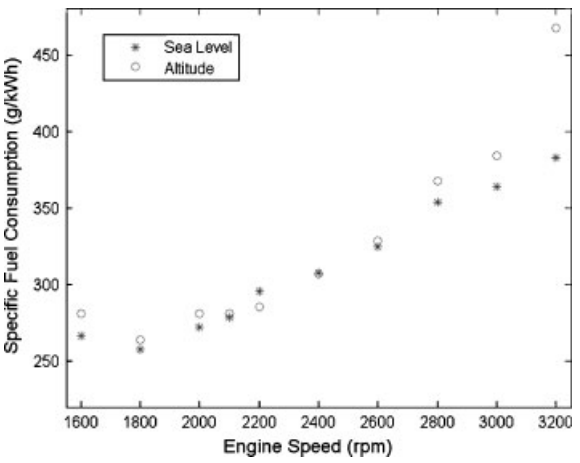

Figure 9. Brake specific fuel consumption ($g\,kWh^{-1}$) for a fixed power output of 1500 W as function of engine speed.

engine speed of 2200 rpm, the engine efficiency changed remarkably little between sea level and at altitude. However, as the engine speed was increased above 2600 rpm the engine became progressively less efficient at altitude than it was at sea level (see Figure 9). At our preferred engine speed of 2200 rpm and a power output of 1500 W, the engine's BSFC at altitude is $280\,g\,kWh^{-1}$.

5.2. Injection timing

In Figures 10 and 11 we present the results of tests at an injection timing of 18° CA BTDC ('Test A'), 13° CA BTDC, then again at 18° CA BTDC ('Test B'). The engine speed was fixed at 2200 rpm.

From Figure 10 it was clear that at 2200 rpm the injection timing has little effect on the fuel consumption. However, as seen in Figure 11, the engine ran hotter at 13° CA BTDC than at 18° CA BTDC both at sea level and at altitude. At altitude, the exhaust gas temperature could be as much as 65°C hotter with the less advanced timing.

This increase in exhaust temperature is likely to be because of a slower combustion due to the reduced air density. Heat that is liberated towards end of the expansion stroke does no useful work

DOI: 10.1002/er

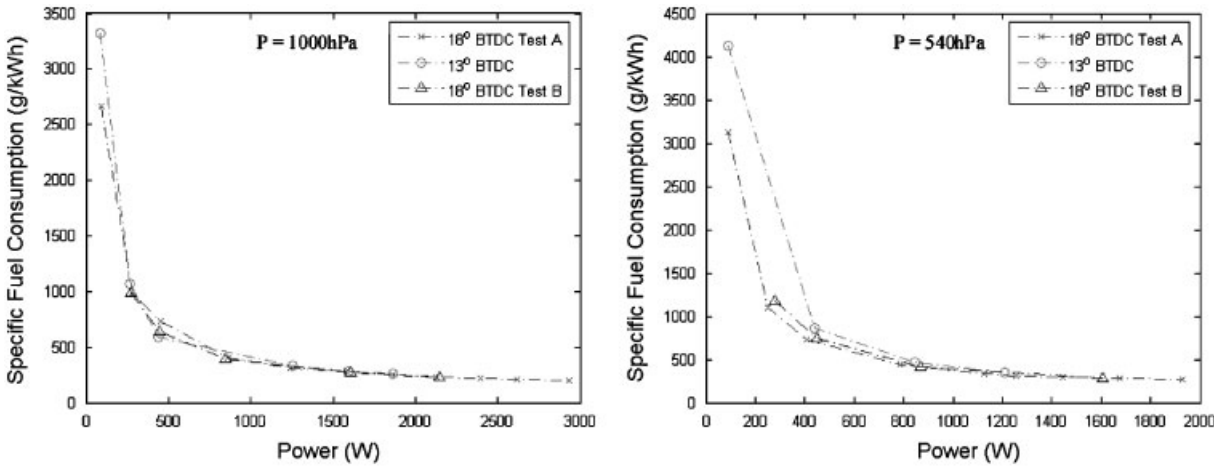

Figure 10. Brake specific fuel consumption at sea level (left) and at altitude (right) at fuel injection timings of 13° and 18° CA BTDC.

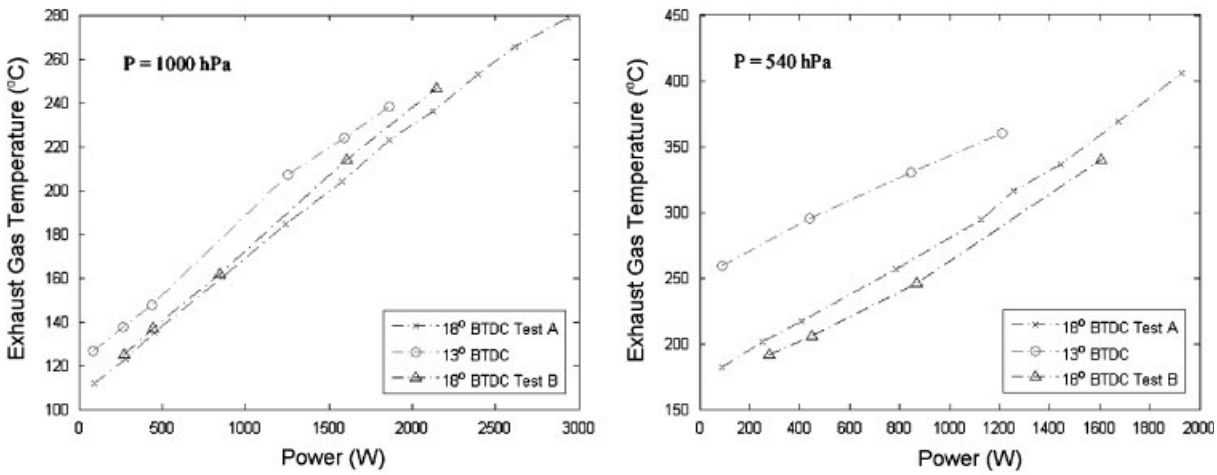

Figure 11. Exhaust gas temperature at sea level (left) and at altitude (right) at fuel injection timings of 13° and 18° CA BTDC.

and only serves to heat up the exhaust valve and pipe [27]. Nevertheless, it is surprising that the injection timing has such a profound effect on the exhaust temperature, while having little or no effect on the fuel consumption.

6. CONCLUSION

Little modification to the Hatz 1B30 engine was required for it to start and run satisfactorily at an altitude of up to 5000 m. Because the maximum power output at a given speed was reduced in direct proportion to the air pressure, so the maximum fuel delivery must also be correspondingly reduced. However, because the air is less dense, there is less working fluid available to do the thermodynamic work and less cooling is available, and so the temperature rise (cylinder head, exhaust gas, etc.) is greatly increased for a given power output. By advancing the start of the fuel delivery timing there is more time for

DOI: 10.1002/er

combustion early in the power stroke, liberating useful work and minimising this increase in exhaust gas temperature.

Allowing for an alternator efficiency of approximately 90%, we find that BSFC of the engine at sea level is consistent with published data. Furthermore, little loss of efficiency, if any, is encountered when the engine is running at high altitude.

An ultracapacitor starting bank has been shown to provide ample cranking current at temperatures as low as -40°C. Both the engine and the starting bank survive temperature cycling to -90°C with no discernable ill effect.

The PLATO power generation system is an innovative and scalable system that can be implemented for remote sites anywhere on the Antarctic plateau and at other high-altitude locations up to 5000 m.

ACKNOWLEDGEMENTS

This research is supported by the Australian Research Council. We thank the UNSW School of Mechanical and Manufacturing Engineering for access to the Internal Combustion Laboratory. Hatz Australia, and in particular Sami Almogoawish, Ian O'Callaghan and Tissa Pathiratna, provided us with the invaluable assistance and generously shared their deep understanding of diesel engines with us. We also thank Jason and Graham Allen for their help in modifying the oil and fuel systems. One of the resistor load banks was generously lent to us by Graeme Arnold and Bob Bell from Swithgear Commissioning & Maintenance Pty Ltd and the other by Ian Davis from Eaton Electric Systems Pty Ltd.

REFERENCES

1. Lüthi D, Le Floch M, Bereiter B, Blunier T, Barnola J, Siegenthaler U, Raynaud D, Jouzel J, Fischer H, Kawamura K, Stocker TF. High-resolution carbon dioxide concentration record 650,000–800,000 years before. *Nature* 2008; **453**:379–382.
2. Storey JWV. Astronomy from Antarctica. *Antarctic Science* 2005; **17**(4):555–560.
3. Yang H, Allen G, Ashley MCB, Bonner CS, Bradley S, Cui X, Everett JR, Feng L, Gong X, Hengst S, Hu S, Jiang Z, Kulesa CA, Lawrence JS, Li Y, Luong-Van D, McCaughrean MJ, Moore AM, Pennypacker C, Qin W, Riddle R, Shang Z, Storey JWV, Sun Z, Suntzeff N, Tothill NFH, Travouillon T, Walker CK, Wang L, Yan J, Yang J, York D, Yuan X, Zhang X, Zhang Z, Zhou X, Zhu Z. The PLATO Dome A site-testing observatory: instrumentation and first results. *PASP* 2009; **121**:174–184.
4. Lawrence JS, Allen GR, Ashley MCB, Bonner C, Bradley S, Cui X, Everett JR, Feng X, Hengst S, Hu J, Jian Z, Kulesa CA, Li Y, Luong-Van D, Moore AM, Pennypacker C, Qin W, Riddle R, Shang Z, Storey JWV, Sun B, Suntzeff N, Tothill NFH, Travouillon T, Walker CK, Wang L, Yan J, Yang J, Yang H, York D, Yuan X, Zhang X, Zhang Z, Zhou X, Zhu Z. The PLATO Antarctic site testing observatory. *Proceedings of SPIE* 2008; **7012**:701227.
5. Lawrence JS, Ashley MCB, Hengst S, Luong-Van DM, Storey JWV, Yang H, Zhou X, Zhu Z. The PLATO Dome A site testing observatory: power generation and control systems. *Review of Scientific Instruments* 2009; **80**:064501.
6. Lawrence JS, Ashley MCB, Burton MG, Cui X, Everett JR, Kenyon SL, Luong-Van D, Moore AM, Storey JWV, Tokovinin A, Travouillon T, Pennypacker C, Wang L, York D. Site testing Dome A, Antarctica. *Proceedings of SPIE* 2006; **6237**:62671L1–62671L9.
7. Tothill NFH, Kulsea CK, Ashley MCB, Bonner C, Everett J, Feng L, Hengst S, Hu J, Jian Z, Lawrence JS, Li Y, Luong-Van D, Moore AM, Pennypacker C, Qin W, Riddle R, Storey JWV, Shang Z, Sun B, Travouillon T, Wang L, Xu Z, Yang H, Yan J, York D, Yuan X, Zhu Z. Astrophysics from Dome A. *EAS Publication Series*: In *Proceedings of the 2nd ARENA Conference*, Potsdam, Germany, Zinnecker H, Rauer H, Epchtein N (eds). EAS Publications Series, vol. 33, 2008; 301–306.
8. Luong-Van DM, Ashley MCB, Everett JR, Lawrence JS, Storey JWV. PLATO control and robotics. *Proceedings of SPIE* 2008; **7019**:70192U.
9. Hengst S, Allen GR, Ashley MCB, Everett JR, Lawrence JS, Luong-Van D, Storey JWV. PLATO Power—a robust, low environmental impact power generation system for the Antarctic plateau. *Proceedings of SPIE* 2008; **7012**:70124E.
10. Available from: http://www.aad.gov.au/weather/aws/dome-a/index.html (January 2009).
11. Lawrence JS, Ashley MCB, Storey JWV. A remote, autonomous laboratory for Antarctica with hybrid power generation. *Australian Journal of Elecrical & Electronic Engineering* 2005; **2**:1–12.
12. Datta BK, Velayutham G, Goud AP. Fuel cell power source for a cold region. *Journal of Power Sources* 2002; **106**:370–376.
13. Available from: http://www.mobil.com/USA-English/Lubes/PDS/NAXXENCVLMOMobil_Delvac_1_5W-40.asp (January 2009).
14. Maurice LQ, Lander H, Edwards T, Harrison III WE. Advanced aviation fuels: a look ahead via a historical perspective. *Fuel* 2001; **80**:747–756.
15. Batchelor G, Moses C, Fletcher R. Impact study on the use of Jet A fuel in military aircraft during operations in Europe; *AGARD Report 801*, 1997.
16. Meloni A, De Santis A, Morelli A, Palangio P, Romeo G, Bozzo E, Caneva G. The geophysical observatory at Terra Nova Bay. *Recent Progress in Antarctic Earth Science TERRAPUB* 1992; 585–588.
17. Available from: http://www.mobil.com/Australia-English/Lubes/PDS/glxxenpvlmomobil1_racing_2t.pdf (January 2009).

18. Product Specification: Jet A-1. *Fuels Technical Services*, BP Australia Pty. Ltd., 2008.
19. Product Specification: BP Automotive Diesel Fuel. *Fuels Technical Services*, BP Australia Pty. Ltd., 2006.
20. Product Specification: BP Antarctic Diesel. *Fuels Technical Services*, BP Australia Pty. Ltd., 2008.
21. Safety Data Sheet: Jet A-1. Shell Company of Australia Ltd., 2005.
22. Material Safety Data Sheet: Jet A-1. *BP Australia Pty. Ltd.*, 2008.
23. Material Safety Data Sheet: Automotive Diesel, *BP Australia Pty. Ltd.*, 2008.
24. Material Safety Data Sheet: BP Antarctic Diesel Fuel (SAB). *BP Australia Pty. Ltd.*, 2008.
25. Assanis D, Fernandes G, Fuschetto J, Filipi Z, McKee H. Impact of military JP-8 fuel on heavy duty diesel engine performance and emissions. *Proceedings of the Institution of Mechanical Engineers*: *Part D* 2007; **221**.
26. Colket M, Edwards T, Williams S, Cernasky NP, Miller DL, Egolfopoulos F, Lindstedt P, Seshadri K, Dryer FL, Law CK, Friend D, Lenhert DB, Pitsch H, Sarofim A, Smooke M, Tsang W. Development of an experimental database and kinetic models for surrogate jet fuels. *AIAA* 2007; 2007–2770.
27. Ricardo HR, Hempson JGG. *The High Speed Internal Combustion Engine*. Blackie: London, U.K., 1968.

DOI: 10.1002/er